

Placing the HIRA Histone Chaperone Complex in the Chromatin Landscape

Nikolay A. Pchelintsev,¹ Tony McBryan,¹ Taranjit Singh Rai,¹ John van Tuyn,¹ Dominique Ray-Gallet,² Geneviève Almouzni,² and Peter D. Adams^{1,*}

¹CR-UK Beatson Labs, Institute of Cancer Sciences, University of Glasgow, Glasgow G61 1BD, UK

²Institut Curie, Centre de Recherche/CNRS, UMR218, Paris 75248, France

*Correspondence: p.adams@beatson.gla.ac.uk
<http://dx.doi.org/10.1016/j.celrep.2013.03.026>

SUMMARY

The HIRA chaperone complex, comprised of HIRA, UBN1, and CABIN1, collaborates with histone-binding protein ASF1a to incorporate histone variant H3.3 into chromatin in a DNA replication-independent manner. To better understand HIRA's function and mechanism, we integrated HIRA, UBN1, ASF1a, and histone H3.3 chromatin immunoprecipitation sequencing and gene expression analyses. Most HIRA-binding sites colocalize with UBN1, ASF1a, and H3.3 at active promoters and active and weak/poised enhancers. At promoters, binding of HIRA/UBN1/ASF1a correlates with the level of gene expression. HIRA is required for deposition of histone H3.3 at its binding sites. There are marked differences in nucleosome and coregulator composition at different classes of HIRA-bound regulatory sites. Underscoring this, we report physical interactions between the HIRA complex and transcription factors, a chromatin insulator and an ATP-dependent chromatin-remodeling complex. Our results map the distribution of the HIRA chaperone across the chromatin landscape and point to different interacting partners at functionally distinct regulatory sites.

INTRODUCTION

The HIRA chaperone complex, comprised of HIRA, UBN1, and CABIN1, collaborates with histone-binding protein ASF1a to incorporate the histone variant H3.3 into chromatin in a DNA replication-independent manner (Loppin et al., 2005; Ray-Gallet et al., 2002; Tagami et al., 2004). HIRA is required for early embryo development (Roberts et al., 2002; Szenker et al., 2012), and histone H3.3 is mutated in human cancer (Schwartzentruber et al., 2012; Wu et al., 2012).

Histone H3.3 is enriched at nucleosomes at transcription start sites (TSSs) of genes, at enhancers, and gene bodies of actively transcribed genes (Ahmad and Henikoff, 2002; Goldberg et al., 2010; Jin et al., 2009). Histone H3.3 contributes to nucleosome destabilization (Jin and Felsenfeld, 2007) and so is thought to facilitate nucleosome dynamics associated with transcription

activation and ongoing transcription. The HIRA protein is required for deposition of histone H3.3 at many of these regions (Goldberg et al., 2010; Ray-Gallet et al., 2011). Consistent with this, HIRA is required for gene activation in some contexts (Dutta et al., 2010; Placek et al., 2009; Yang et al., 2011). Interestingly, the HIRA complex and its orthologs, together with histone H3.3, are also involved in chromatin silencing (Sherwood et al., 1993; van der Heijden et al., 2007).

The distribution of the HIRA chaperone complex across the epigenome is not known, and there is a paucity of partner proteins known to participate in its diverse functions. To overcome this, we performed integrated chromatin immunoprecipitation sequencing (ChIP-seq) and gene expression analyses and used these analyses to identify proteins that physically interact with the HIRA complex in chromatin regulation.

RESULTS

Analysis of Genome-wide Distribution of HIRA, UBN1, ASF1a, and Histone H3.3

To gain insight into the function and regulation of the HIRA chaperone at distinct genomic sites, we performed ChIP-seq of endogenous HIRA, UBN1, and ASF1a in human HeLa cells. Analysis of the aligned reads yielded 8,296 HIRA peaks, 62,712 UBN1 peaks, and 64,550 ASF1a peaks, compared to input DNA. Of HIRA peaks, 74% (6,147 out of 8,296) were co-occupied by both UBN1 and ASF1a (Figure 1A; Table S1). To confirm these results, we performed anti-HIRA ChIP followed by quantitative PCR (ChIP-qPCR) at a single co-occupied HIRA/UBN1/ASF1a peak and flanking regions. This analysis confirmed enrichment of HIRA at the peak, relative to the flanking regions (Figure 1B). Specific enrichment at this site was also observed with antibodies to UBN1 and ASF1a (Figure 1C) as well as with four individual monoclonal antibodies to HIRA (Figure S1A) by ChIP-qPCR. Indeed, across the whole genome, HIRA-binding regions were coincident with UBN1 and ASF1a-binding regions (Figure 1D). We also performed ChIP of HIRA followed by semi-qPCR at nine distinct locations selected at random from the list of 6,147 HIRA/UBN1/ASF1a peaks; all nine regions demonstrated enrichment in HIRA ChIP compared to nonspecific antibody (anti-GFP) (Figure 1E; Table S2). Taken together, these data show that the core HIRA complex and ASF1a co-occupy at least several thousand discrete sites across the genome of proliferating human cells.

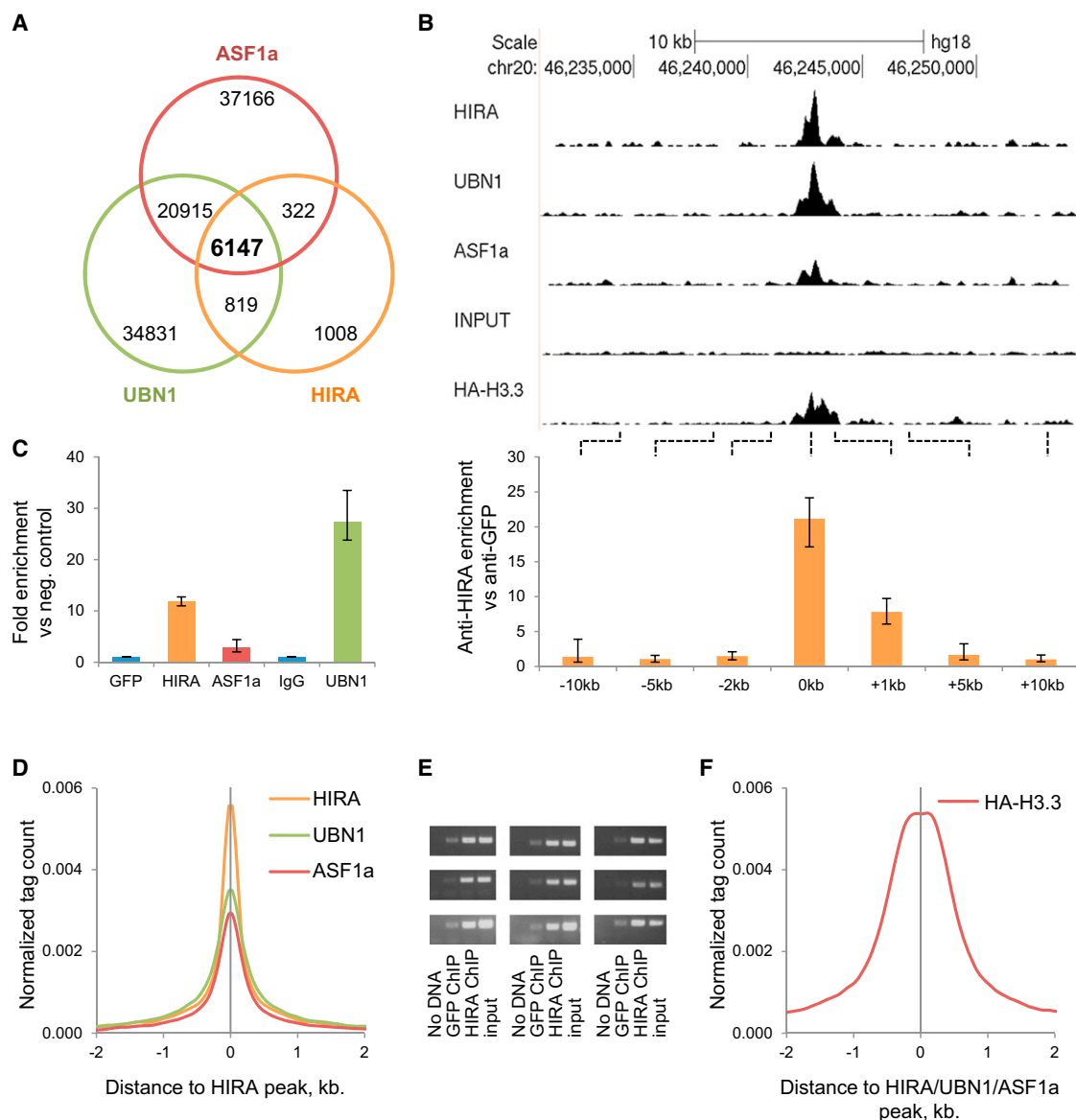


Figure 1. ChIP-Seq of HIRA, UBN1, and ASF1a Defines HIRA Complex and ASF1a-Binding Sites

(A) Venn diagram of overlap between HIRA, UBN1 and ASF1a peaks reveals a subset of 6,147 co-occupied regions. See also [Table S1](#).
 (B) Representative HIRA, UBN1, ASF1a, and HA-H3.3 ChIP-seq tracks and ChIP-qPCR validation of HIRA enrichment at peak compared to flanking regions. Error bars show SEs. See also [Table S2](#).
 (C) ChIP-qPCR validation of the complex-binding region shown in (B) using a cocktail of monoclonal antibodies to HIRA or ASF1a or a rabbit polyclonal antibody to UBN1. Error bars show SEs. neg., negative. See also [Figure S1A](#) and [Table S2](#).
 (D) Normalized density of ChIP-seq tags of HIRA, UBN1, and ASF1a in a 4 kb window centered on a composite of all HIRA peaks.
 (E) ChIP-PCR validation of nine different HIRA-binding regions identified by ChIP-seq. See also [Table S2](#).
 (F) Normalized density of ChIP-seq tags of HA-H3.3 in a 4 kb window centered on a composite of all HIRA/UBN1/ASF1a peaks.

Although HIRA is required for accumulation of histone H3.3 at many sites throughout the genome ([Dutta et al., 2010](#); [Goldberg et al., 2010](#); [Placek et al., 2009](#); [Yang et al., 2011](#)), the genomic distribution of newly deposited histone H3.3 and the HIRA complex (as well as ASF1a) have not been directly compared. Therefore, we assessed the genome-wide distribution of the newly incorporated histone H3.3 by anti-HA ChIP-

seq on HeLa cells after a short pulse of HA-histone H3.3 expression (less than 13 hr). By this approach, we identified 110,213 sites of HA-H3.3 deposition across the genome. Strikingly, 86% of all HIRA-binding sites and 95% of co-occupied HIRA/UBN1/ASF1a sites were also enriched for HA-H3.3. Moreover, across the whole genome, co-occupied HIRA/UBN1/ASF1a sites were generally coincident with peaks of HA-H3.3

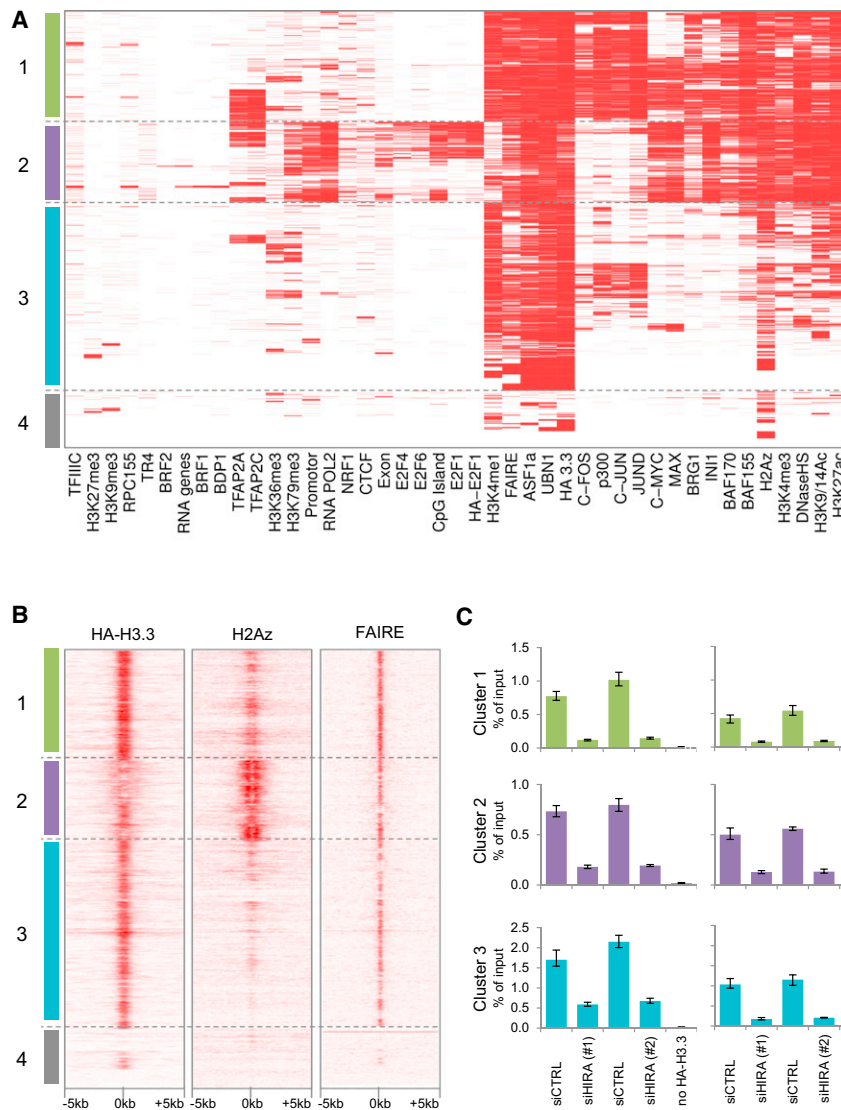


Figure 2. HIRA Binds to Chromatin at Four Distinct Classes of Genomic Loci

(A) Unsupervised clustering identifies four distinct clusters of HIRA peaks.

(B) Heatmaps of normalized density of ChIP-seq tags of HA-H3.3, H2Az, and FAIRE in a 10 kb window centered on a HIRA peak. HIRA peaks are arranged in the same order as in (A) and grouped in four clusters. See also Figure S1.

(C) siRNA-mediated knockdown of HIRA impairs HA-H3.3 incorporation at representative regions of clusters 1, 2, and 3 as measured by HA ChIP-qPCR. Error bars show SEs. CTRL, control. See also Figure S2A for confirmation of efficient protein knockdown and Table S2 for regions location.

deposition (Figures 1B and 1F). Furthermore, peaks of histone H3.3 were more pronounced at peaks of HIRA/UBN1/ASF1a than elsewhere in the genome (Figure S1B). These results support the view that the HIRA complex and ASF1a collaborate to deposit histone H3.3 at their specific colocalization sites.

HIRA Binds to Chromatin at Four Distinct Classes of Genomic Loci

To further characterize chaperone function, we determined the distribution of regions co-occupied by HIRA, UBN1, and ASF1a between promoter, genic and intergenic regions: 22% of the 6,147 HIRA/UBN1/ASF1a peaks mapped to gene promoters and the rest to either gene body (38%) or intergenic regions (40%) (Figures S1C and S1D).

To better characterize HIRA's binding across the genome, we performed unsupervised clustering of all 8,296 HIRA-binding sites according to their overlap with UBN1, ASF1a, HA-H3.3, and other chromatin proteins and genomic features annotated

in HeLa cells in publicly available databases. In addition, we performed formaldehyde-assisted isolation of regulatory elements (FAIRE) to identify accessible regions of DNA in the same cells and incorporated this into the analysis (Table S1). This analysis separated HIRA-binding sites into four distinct clusters: 1, 2, 3, and 4 (Figure 2A). Clusters 1–3 were comprised largely of HIRA peaks co-occupied by UBN1 and ASF1a, whereas cluster 4 was predominantly comprised of HIRA-only peaks, lacking UBN1 and ASF1a.

Cluster 1 is enriched in H3K4me1/H3K4me3, H3K27ac, H2Az, p300, and transcription factor c-MYC (Figure 2A). Almost all regions in this cluster are also FAIRE positive and DNase hypersensitive (DNaseHS) and exhibit very low overlap with RNA polymerase II, CpG islands, or promoters of annotated genes. Such a binding pattern is best associated with active enhancers (Ernst et al., 2011; Heintzman et al., 2009; Rada-Iglesias

et al., 2011), suggesting that cluster 1 represents HIRA/UBN1/ASF1a binding at these regulatory elements.

Cluster 2 shows a strong overlap with gene promoters, RNA polymerase II, CpG islands, H2Az, H3K4me3 (but not H3K4me1), H3K27ac, and transcription factor c-MYC (Figure 2A). Almost all regions in this cluster are FAIRE positive and DNaseHS. This signature is most consistent with promoters of actively transcribed genes (Ernst et al., 2011; Heintzman et al., 2009; Rada-Iglesias et al., 2011).

Cluster 3 is enriched in H3K4me1, but compared to cluster 1, shows less overlap with p300, H3K27ac, and c-MYC and less DNaseHS and FAIRE (Figure 2A). Moreover, cluster 3 shows minimal overlap with promoters, CpG islands, and RNA polymerase II. Consequently, cluster 3 is most consistent with weak or poised enhancers (Ernst et al., 2011; Heintzman et al., 2009; Rada-Iglesias et al., 2011).

Cluster 4 is comprised largely of the 1,008 genomic sites that bind HIRA, but neither UBN1 nor ASF1a (HIRA-only peaks)

(Figures 1A and 2A). Relaxing the stringency of the algorithm for calling ASF1a and UBN1 peaks failed to generate overlap between UBN1 and ASF1a peaks and all the HIRA peaks (Figure S1E). Also, independent reanalysis of read numbers confirmed that those HIRA peaks that scored negative for both ASF1a and UBN1 showed only very few reads in UBN1 and ASF1a ChIPs at these regions (Figure S1F). These analyses support the notion that these apparent HIRA-only peaks genuinely lack enrichment of UBN1 and ASF1a and so are qualitatively distinct from the co-occupied HIRA/UBN1/ASF1a peaks. Consistent with this idea, unlike the HIRA/UBN1/ASF1a-bound regions of the genome, HIRA-only peaks were largely FAIRE and DNaseHS negative, lacked active histone marks (H3K4me3, H3K27ac, and H3K9/14ac) (Figures 2A and S1G), and overlapped poorly with many chromatin regulatory proteins analyzed as part of the ENCODE project (Figure S1H; Table S3). Based on the analysis in Figure 2A, a large proportion of cluster 4 HIRA-binding sites contains detectable H2Az, but a more quantitative analysis, evaluating the number of reads and not simply the presence or absence of binding, showed these sites to be very poor binders of H2Az (Figure 2B). Most surprisingly, in striking contrast to HIRA/UBN1/ASF1a peaks, the HIRA-only sites were also largely depleted of histone H3.3 (Figures 2A, S1G, and S1I). Taken together, these data suggest that HIRA binds to some sites in the genome in the absence of UBN1 and ASF1a and without steady-state enrichment of histone H3.3. Together, this indicates a very different, but currently unknown, function for HIRA at these sites.

To gain further insight into HIRA clusters 1–4 we also plotted quantitative heatmaps of the abundance of newly synthesized HA-histone H3.3, H2Az, and FAIRE accessibility, 5 kb either side of the centered HIRA peak, and with the HIRA-binding loci vertically ordered as in Figures 2A and 2B. These plots underscored the difference between clusters 1–4. At cluster 2, as expected for promoters, HA-H3.3 and H2Az both showed a bimodal distribution, indicative of H3.3/H2Az-containing nucleosomes either side of the nucleosome-free, FAIRE-positive TSS (Jin et al., 2009). Interestingly, the nucleosome-free region was positioned very close to the centered HIRA peak (Figure 2B). Thus, at promoters, HIRA/UBN1/ASF1a is essentially localized to the nucleosome-free TSS. Although the active enhancers in cluster 1 were also characterized by coincident HIRA/UBN1/ASF1a and FAIRE peaks, the distribution of HA-H3.3 and H2Az was quite different from the promoters in cluster 2 (Figure 2B). Cluster 1 HIRA/UBN1/ASF1a peaks were less rich in H2Az, and the bimodal distribution of HA-H3.3 and H2Az was less apparent. The weak/poised enhancers of cluster 3 were also characterized by coincident HIRA/UBN1/ASF1a, FAIRE, and HA-H3.3 peaks (Figure 2B). As at cluster 1, the HA-H3.3 was localized to a monomodal, not bimodal, peak. There was relatively little H2Az at cluster 3.

Knockdown of HIRA decreased total incorporation of histone H3.3 into chromatin, as judged by total chromatin-bound (insoluble in Triton X-100) histone H3.3 and total DNA coprecipitated in anti-HA-H3.3 ChIP (Figures S2A and S2B). At specific regions, knockdown of HIRA specifically blocked binding of ectopically expressed epitope-tagged H3.3 at TSSs and promoters (cluster 2) (Figures 2C and S2B), with a much lesser effect on total

endogenous H3 (H3.1, H3.2, and H3.3) at the same sites (Figure S2B). Similarly, loss of HIRA resulted in greatly reduced incorporation of histone H3.3 at cluster 1 and 3 enhancer regions (Figure 2C).

These results indicate that the HIRA complex and ASF1a colocalize with histone H3.3 at diverse regulatory elements throughout the genome (active promoters, strong enhancers, and weak/poised enhancers) and are required for deposition of H3.3 at these sites. Significantly, the localization of histone H3.3 and H2Az differs quantitatively and qualitatively between these different classes of HIRA/UBN1/ASF1a-bound regulatory elements.

Binding of HIRA/UBN1/ASF1a at TSSs Correlates with Gene Expression

The previous comparison of HIRA binding to nucleosome composition and positioning (Figure 2B) suggested that cluster 2 is comprised of HIRA/UBN1/ASF1a bound to gene promoter TSSs. Indeed, when HIRA, UBN1, and ASF1a binding was analyzed at a composite of all genes, the three components were found to bind just upstream of the TSS, coincident with the FAIRE-positive nucleosome-free region between the H3.3/H2Az nucleosomes (Figures 3A and 3B). The composite plot in Figure 3A reflects the average distribution at individual genes (Figure 3C). Significantly, the complex was markedly enriched at the promoters of highly expressed genes but almost absent from the promoters of repressed genes (Figure 3D), demonstrating a positive correlation between HIRA/UBN1/ASF1a binding and gene expression level. In this respect, HIRA/UBN1/ASF1a binding was very similar to H3.3, H2Az, and FAIRE accessibility (Figure 3E). Taken together, these results show that a proportion of the HIRA/UBN1/ASF1a complex is localized to TSSs of highly expressed genes.

Binding Partners of HIRA Complex and ASF1a

Figure 2A reveals a marked overlap between HIRA/UBN1/ASF1a-binding sites and binding of transcription factors and transcription regulators. Strikingly, 76% of HIRA/UBN1/ASF1a peaks colocalize with at least one protein from four families: human SWI/SNF ATP-dependent chromatin-remodeling complexes (BRG1, INI1, BAF155, and BAF170); AP-1 (c-FOS, c-JUN, and JUND [clusters 1 and 3]); c-MYC/MAX (clusters 1 and 2); and TFAP2 (TFAP2A and TFAP2C [clusters 1 and 2]) (Figures 2A and 4A; Table S3). The most robust overlap was observed with various members of the SWI/SNF family of chromatin remodelers. Specifically, 57%, 41%, 41%, and 36% of HIRA/UBN1/ASF1a peaks overlapped with BAF155, BAF170, INI1, and BRG1, respectively (Table S3). This overlap was particularly marked at active enhancers and promoters (clusters 1 and 2, respectively) (Figure 2A). These transcription regulators represent candidate HIRA/UBN1/ASF1a-bound regulatory partners.

To confirm whether these candidates for HIRA/UBN1/ASF1a-binding partners identified by ChIP-seq are bona fide interacting proteins, we tested specific interactions by immunoprecipitation-western blot analysis. Transcription factors c-MYC, c-JUN, GTF2I (a multifunctional promoter-binding transcription factor; Roy, 2012), chromatin remodelers of the SWI/SNF family (BRG1, BRM, and INI1), and chromatin insulator CTCF (enriched

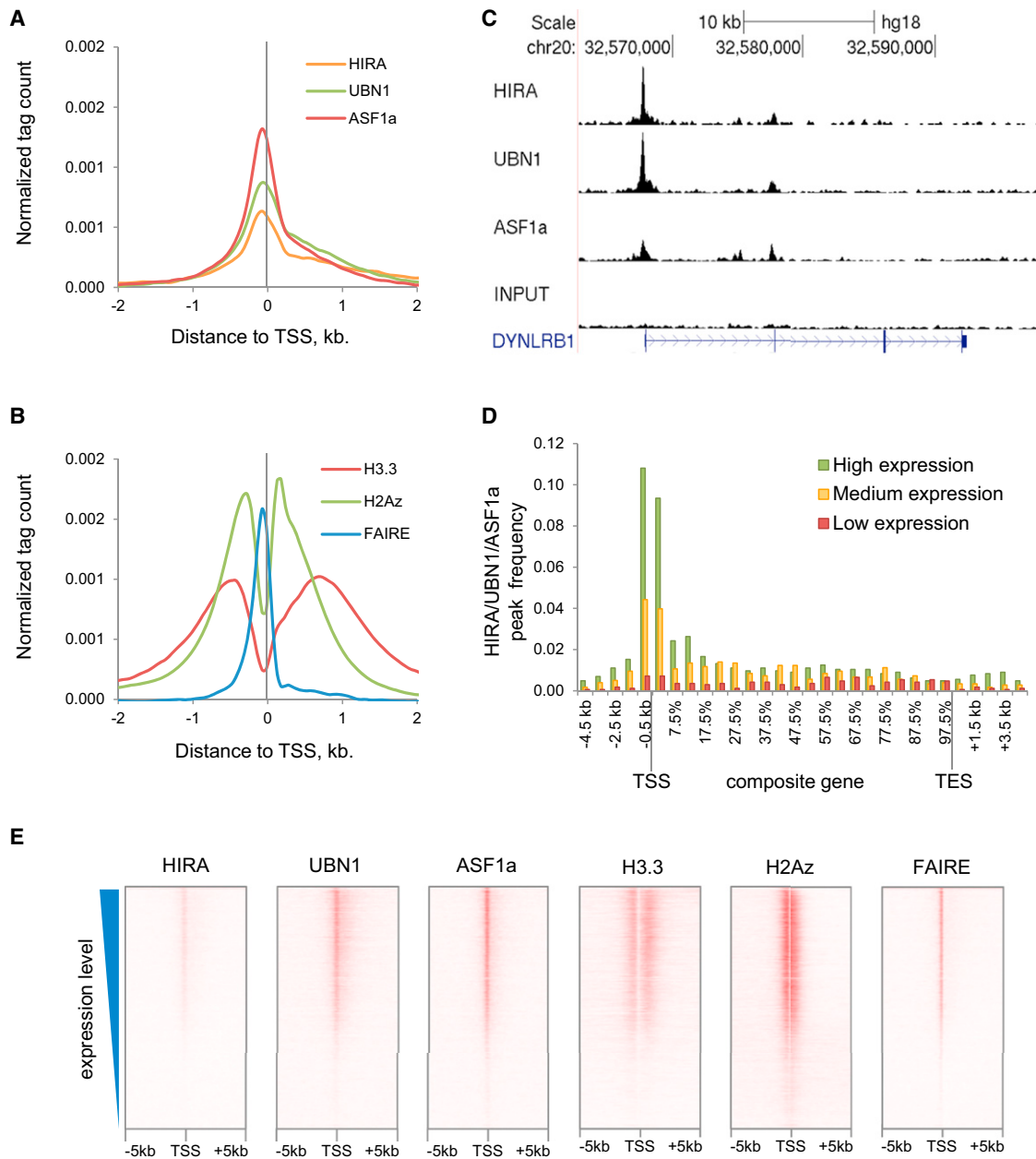


Figure 3. HIRA Complex and ASF1a Are Enriched at the Nucleosome-free Region of TSSs of Highly Expressed Genes

(A) Normalized density of ChIP-seq tags of HIRA, UBN1, and ASF1a in a 4 kb window of a composite promoter centered on TSSs of all genes.

(B) Normalized density of ChIP-seq tags of H3.3, H2Az, and FAIRE in a 4 kb window of a composite promoter centered on TSS of all genes.

(C) Example of characteristic distribution of HIRA, UBN1, and ASF1a across the DYNLRB1 gene. chr20, chromosome 20.

(D) Composite distribution of co-occupied HIRA/UBN1/ASF1a peaks across high-, medium-, or low-expressed genes. Probes on the Affymetrix expression array were rank ordered by average expression level in proliferating HeLa cells. Probes were mapped to Ensembl genes and the top (high)-, bottom (low)-, and middle (medium)-expressed 2,000 genes selected. HIRA/UBN1/ASF1a peak frequency across a composite gene assembled from each group of 2,000 genes was plotted. The x axis shows the position along the gene, where the distance between TSSs and transcription end sites (TESs) is in percentage (%) of gene length, and regions upstream of TSSs and downstream of TESs are in base pairs.

(E) Heatmaps of normalized density of ChIP-seq tags of HIRA, UBN1, ASF1a, H3.3, H2Az, and FAIRE in a 10 kb window centered on TSSs. TSSs are rank ordered according to the expression level of the corresponding transcript.

in clusters 1 and 2; Figure 2A) were all specifically coprecipitated with endogenous HIRA from HeLa lysates, whereas an abundant chromatin-binding protein MCM2 and transcription factor

TCF4 were not (Figure 4B). The interaction between HIRA and BRG1 was additionally confirmed using ectopically expressed epitope-tagged proteins (Figure 4C).

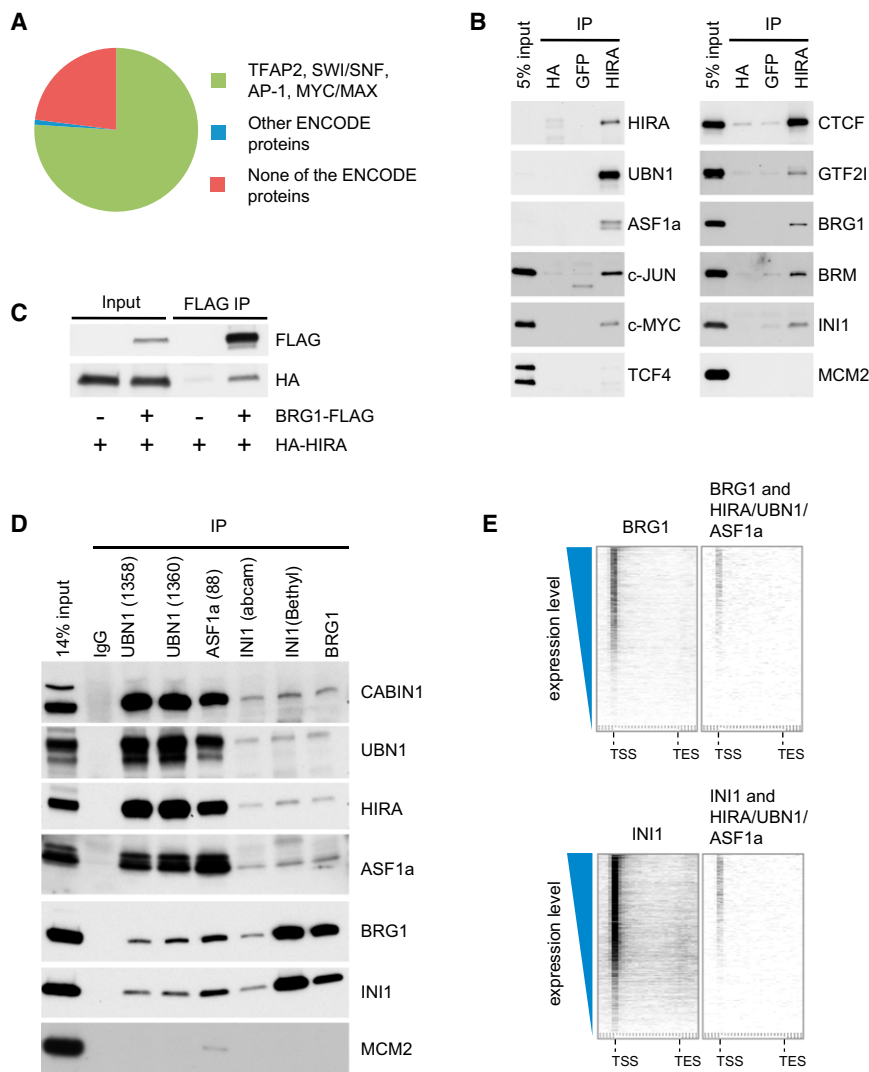


Figure 4. Genomic Overlap and Functional Interaction between HIRA/UBN1/ASF1a and BRG1/INI1

(A) Overlap between HIRA/UBN1/ASF1a peaks and various proteins studied under the ENCODE project. See also Table S3.

(B) Immunoprecipitation (IP) of endogenous HIRA from nuclear lysates coprecipitates other members of the chaperone complex (UBN1, ASF1a) as well as transcription factors (c-JUN, c-MYC, GTF2I), members of SWI/SNF chromatin remodelers (BRG1, BRM, INI1), and CTCF, but not TCF4 or MCM2. See also Figure S3.

(C) Coprecipitation of ectopically expressed epitope-tagged HA-HIRA and FLAG-BRG1.

(D) Coprecipitation of endogenous members of UBN1, ASF1a, CABIN1, and SWI/SNF complex (BRG1/INI1) from nuclear lysates.

(E) HIRA/UBN1/ASF1a colocalizes with BRG1 and INI1 at the TSS of highly expressed genes. Distribution of genic BRG1, BRG1-positive HIRA/UBN1/ASF1a, INI1, and INI1-positive HIRA/UBN1/ASF1a peaks plotted against the normalized gene coordinate (x axis), with genes sorted according to their level of expression in HeLa cells. Gray windows show at least 2-fold enrichment of HIRA/UBN1/ASF1a relative to input.

Antibodies to UBN1 and ASF1a also coprecipitated subunits of SWI/SNF, BRG1, and INI1 (Figure 4D). Conversely, antibodies to BRG1 and INI1 coprecipitated HIRA, UBN1a, ASF1a, and CABIN1 (Figure 4D). Confirming appropriate specificity and sensitivity of these assays, only antibodies to ASF1a coprecipitated MCM2 (Figure 4D). The DNA replication-independent chromatin regulators HIRA, UBN1, INI1, and BRG1 do not interact with the DNA replication helicase MCM2, whereas ASF1a does bind to MCM2 due to its HIRA/UBN1/CABIN1-independent role in DNA replication-coupled nucleosome assembly (Groth et al., 2007). Coprecipitation of HIRA, BRG1, and INI1 was largely resistant to denaturation of DNA-protein interactions by ethidium bromide in the lysis buffer and occurred even after digestion of chromatin to predominantly mono- and dinucleosomes (Figure S3A), suggesting that the coprecipitation does not reflect an indirect interaction mediated by long-range chromatin structure.

To verify close physical proximity between HIRA and the BRG1/INI1 complex, we used the proximity ligation assay

to several proteins not known to interact with HIRA (DNMT1, MCM2, UACA, ATRX, XRN1, MBD2, LSH, and EDC4; Figures S3B and S3C). In sum, targeted immunoprecipitation-western blot analyses and PLAs verified many of the physical interactions indicated by ChIP-seq. Of particular note, BRG1/INI1 appears to physically interact, directly or indirectly, with multiple members of the HIRA complex and ASF1a.

To further investigate the HIRA/UBN1/ASF1a and BRG1/INI1 interaction, we more closely compared the genome-wide distribution of co-occupied HIRA/UBN1/ASF1a-binding sites with previously published data describing the genome-wide distribution of BRG1 and INI1, also in HeLa cells (Euskirchen et al., 2011). This analysis revealed coincident HIRA/UBN1/ASF1a and BRG1 peaks, overlapping with H3.3-containing nucleosomes (e.g., Figure S3D). Like HIRA/UBN1/ASF1a, BRG1/INI1 has been previously reported to be enriched at many gene TSSs, and unsupervised clustering revealed marked overlap of HIRA/UBN1/ASF1a and BRG1/INI1 at active gene promoters (cluster 2, Figure 2A). Indeed, at genic regions, colocalization between

HIRA/UBN1/ASF1a and BRG1/INI1 was most prominent at the TSS of highly expressed genes (Figure 4E).

DISCUSSION

More than 6,000 loci are co-occupied by HIRA, UBN1, and ASF1a across the genome. We also find a striking colocalization with histone H3.3, its preferred deposition substrate, at 95% (5,867) of these sites. HIRA contributes to total deposition of histone H3.3 in the genome and at all its specific binding sites tested. Co-occupied HIRA, UBN1, and ASF1a-binding sites occur at three main regulatory elements; namely, promoters of active genes and active and weak/poised enhancers. At active promoters, histone H3.3 and H2Az both show a bimodal distribution reflecting H3.3/H2Az-containing nucleosomes either side of the TSS. However, active and weak/poised enhancers exhibit monomodal H3.3 and H2Az peaks. Active enhancers bind more H3.3 and H2Az than weak/poised enhancers. These results extend previous studies to further distinguish between different local nucleosome structures at distinct regulatory elements (Ernst et al., 2011; Heintzman et al., 2009; Rada-Iglesias et al., 2011).

At gene promoters, HIRA, UBN1, and ASF1a bind at the FAIRE-positive “nucleosome-free” region just upstream of the TSS, and binding of all three factors, as well as H2Az and H3.3 either side of the TSS, shows a striking correlation with gene expression. The nucleosome-free region is thought to dynamically cycle between the nucleosome-bound and unbound state (Jin et al., 2009). The chaperone complex likely contributes to these dynamics. Interestingly, whereas histone H3.3 accumulates at the 3' end of gene bodies of actively transcribed genes (Goldberg et al., 2010), we did not observe enrichment of HIRA/UBN1/ASF1a at these regions (Figures 3C and 3D). This suggests that HIRA/UBN1/ASF1a is more stably bound to TSSs, where there is perhaps a more long-term requirement in anticipation of transcription initiation, compared to gene bodies where it is only transiently required in conjunction with transcription-coupled nucleosome reassembly.

Surprisingly, HIRA binds to at least 1,000 sites across the genome, in the absence of UBN1 and ASF1a (HIRA-only-binding sites). The chromatin landscape of these HIRA-only sites is very different from combined HIRA/UBN1/ASF1a-binding sites. Most notably, HIRA-only-binding sites are not enriched in H3.3, suggesting a quite different function for HIRA in the absence of UBN1 and ASF1a. To date, these 1,000 HIRA-only-binding sites have not revealed other features in common, so the nature of this function is currently unknown.

We identified proteins that bind directly or indirectly to ASF1a and/or the HIRA complex, namely c-JUN, c-MYC, GTF2I, CTCF, and BRG1/INI1. Their interaction with the H3.3 chaperone is likely to direct and modulate histone chaperone activity. A physical interaction between the HIRA complex and ASF1a and BRG1 and INI1 is consistent with previous reports that have linked members of the HIRA complex and SWI/SNF ATP-dependent chromatin-remodeling factors in model organisms (Dimova et al., 1999; Konev et al., 2007; Moshkin et al., 2002). Our ChIP-seq analysis indicates that the HIRA/UBN1/ASF1a interaction with BRG1/INI1 likely occurs preferentially at active promoters

and enhancers, compared to weak/poised enhancers. This illustrates a general conclusion of our analysis that the nucleosome and coregulator composition of the chaperone's binding sites varies considerably between the different types of regulatory elements. Presumably, different networks of physical and functional interactions, involving HIRA/UBN1/ASF1a, dictate the distinct functional properties of active promoters and active and weak/poised enhancers.

EXPERIMENTAL PROCEDURES

See [Extended Experimental Procedures](#) for more details and references.

HIRA, UBN1, and ASF1a ChIP

HeLa cells were crosslinked with 1.5 mM EGS in PBS for 45 min at room temperature, followed by treatment with 1% formaldehyde for 15 min. After quenching with glycine, the cells were harvested and sonicated to produce soluble chromatin with DNA fragments in the range of 150–300 bp. For ChIP, this fragmented chromatin was incubated with antibodies to HIRA, UBN1, or ASF1a preimmobilized on Dynabeads.

Histone ChIP

HeLa cells were crosslinked with 1% formaldehyde in DMEM for 15 min. After that, the procedure was similar to HIRA ChIP.

FAIRE

FAIRE DNA was purified from the same inputs that were used for HA-H3.3 ChIPs as described previously by Giresi et al. (2007). Briefly, input sample was extracted twice with phenol-chloroform-isoamyl alcohol mixture, and FAIRE DNA was recovered from the aqueous phase using QIAGEN PCR clean-up kit.

Massively Parallel Sequencing and Data analysis

Libraries were prepared from 10 to 20 ng of ChIP or input DNA using Illumina ChIP-seq kit according to the manufacturer's instructions, and the resulting libraries were sequenced on GAIIx to yield about 30 million raw reads. ChIP-seq or input reads were mapped to the human genome (hg18) using the Bowtie alignment software. Only unique reads mapping to a single location were retained. Determination of enriched regions was performed using the USeq package, and reads were visualized using the UCSC browser. Results presented are analyzed from a single ChIP-seq reaction of each of UBN1 and ASF1a, but results are representative of two independent ChIP-seq reactions for HIRA.

ACCESSION NUMBERS

The Gene Expression Omnibus accession number for the data reported in this paper is GSE45025. This data series includes the following subseries: HIRA, UBN1, and ASF1a ChIP-seq (GSE45024); newly synthesized HA-H3.3 ChIP-seq and corresponding FAIRE-seq (GSE45023); and expression microarrays of siHIRA- and scrambled siRNA-treated HeLa (GSE45022).

SUPPLEMENTAL INFORMATION

Supplemental Information includes three figures, three tables, and Extended Experimental Procedures and can be found with this article online at <http://dx.doi.org/10.1016/j.celrep.2013.03.026>.

LICENSING INFORMATION

This is an open-access article distributed under the terms of the Creative Commons Attribution-NonCommercial-No Derivative Works License, which permits non-commercial use, distribution, and reproduction in any medium, provided the original author and source are credited.

ACKNOWLEDGMENTS

We thank Pawel Herzyk, Julie Galbraith, and William Clark for DNA sequencing, David Strachan and Lynn McGarry for image analysis, and Sarah Kinkley, Adam Woolfe, David Vetrie, and Koorosh Koorfi for critical discussions. We thank members of the Adams laboratory and NIA program project members for critical discussions. Work in G.A.'s lab was supported by la Ligue Nationale contre le Cancer (Equipe labellisée Ligue). Work in the Adams laboratory was funded by CR-UK program project, C10652/A10250, and program project NIA AG031862-02.

Received: December 19, 2011

Revised: March 4, 2013

Accepted: March 19, 2013

Published: April 18, 2013

REFERENCES

- Ahmad, K., and Henikoff, S. (2002). The histone variant H3.3 marks active chromatin by replication-independent nucleosome assembly. *Mol. Cell* 9, 1191–1200.
- Dimova, D., Nackerdien, Z., Furgeson, S., Eguchi, S., and Osley, M.A. (1999). A role for transcriptional repressors in targeting the yeast Swi/Snf complex. *Mol. Cell* 4, 75–83.
- Dutta, D., Ray, S., Home, P., Saha, B., Wang, S., Sheibani, N., Tawfik, O., Cheng, N., and Paul, S. (2010). Regulation of angiogenesis by histone chaperone HIRA-mediated incorporation of lysine 56-acetylated histone H3.3 at chromatin domains of endothelial genes. *J. Biol. Chem.* 285, 41567–41577.
- Ernst, J., Kheradpour, P., Mikkelsen, T.S., Shores, N., Ward, L.D., Epstein, C.B., Zhang, X., Wang, L., Issner, R., Coyne, M., et al. (2011). Mapping and analysis of chromatin state dynamics in nine human cell types. *Nature* 473, 43–49.
- Euskirchen, G.M., Auerbach, R.K., Davidov, E., Gianoulis, T.A., Zhong, G., Rozowsky, J., Bhardwaj, N., Gerstein, M.B., and Snyder, M. (2011). Diverse roles and interactions of the SWI/SNF chromatin remodeling complex revealed using global approaches. *PLoS Genet.* 7, e1002008.
- Fredriksson, S., Gullberg, M., Jarvius, J., Olsson, C., Pietras, K., Gústafsdóttir, S.M., Ostman, A., and Landegren, U. (2002). Protein detection using proximity-dependent DNA ligation assays. *Nat. Biotechnol.* 20, 473–477.
- Giresi, P.G., Kim, J., McDaniel, R.M., Iyer, V.R., and Lieb, J.D. (2007). FAIRE (Formaldehyde-Assisted Isolation of Regulatory Elements) isolates active regulatory elements from human chromatin. *Genome Res.* 17, 877–885.
- Goldberg, A.D., Banaszynski, L.A., Noh, K.M., Lewis, P.W., Elsaesser, S.J., Stadler, S., Dewell, S., Law, M., Guo, X., Li, X., et al. (2010). Distinct factors control histone variant H3.3 localization at specific genomic regions. *Cell* 140, 678–691.
- Groth, A., Corpet, A., Cook, A.J., Roche, D., Bartek, J., Lukas, J., and Almouzni, G. (2007). Regulation of replication fork progression through histone supply and demand. *Science* 318, 1928–1931.
- Heintzman, N.D., Hon, G.C., Hawkins, R.D., Kheradpour, P., Stark, A., Harp, L.F., Ye, Z., Lee, L.K., Stuart, R.K., Ching, C.W., et al. (2009). Histone modifications at human enhancers reflect global cell-type-specific gene expression. *Nature* 459, 108–112.
- Jin, C., and Felsenfeld, G. (2007). Nucleosome stability mediated by histone variants H3.3 and H2A.Z. *Genes Dev.* 21, 1519–1529.
- Jin, C., Zang, C., Wei, G., Cui, K., Peng, W., Zhao, K., and Felsenfeld, G. (2009). H3.3/H2A.Z double variant-containing nucleosomes mark 'nucleosome-free regions' of active promoters and other regulatory regions. *Nat. Genet.* 41, 941–945.
- Konev, A.Y., Tribus, M., Park, S.Y., Podhraski, V., Lim, C.Y., Emelyanov, A.V., Vershilova, E., Pirrotta, V., Kadonaga, J.T., Lusser, A., and Fyodorov, D.V. (2007). CHD1 motor protein is required for deposition of histone variant H3.3 into chromatin in vivo. *Science* 317, 1087–1090.
- Loppin, B., Bonnefoy, E., Anselme, C., Laurençon, A., Karr, T.L., and Couble, P. (2005). The histone H3.3 chaperone HIRA is essential for chromatin assembly in the male pronucleus. *Nature* 437, 1386–1390.
- Moshkin, Y.M., Armstrong, J.A., Maeda, R.K., Tamkun, J.W., Verrijzer, P., Kennison, J.A., and Karch, F. (2002). Histone chaperone ASF1 cooperates with the Brahma chromatin-remodelling machinery. *Genes Dev.* 16, 2621–2626.
- Placek, B.J., Huang, J., Kent, J.R., Dorsey, J., Rice, L., Fraser, N.W., and Berger, S.L. (2009). The histone variant H3.3 regulates gene expression during lytic infection with herpes simplex virus type 1. *J. Virol.* 83, 1416–1421.
- Rada-Iglesias, A., Bajpai, R., Swigut, T., Bruggmann, S.A., Flynn, R.A., and Wysocka, J. (2011). A unique chromatin signature uncovers early developmental enhancers in humans. *Nature* 470, 279–283.
- Ray-Gallet, D., Quivy, J.P., Scamps, C., Martini, E.M., Lipinski, M., and Almouzni, G. (2002). HIRA is critical for a nucleosome assembly pathway independent of DNA synthesis. *Mol. Cell* 9, 1091–1100.
- Ray-Gallet, D., Woolfe, A., Vassias, I., Pellentz, C., Lacoste, N., Puri, A., Schultz, D.C., Pchelintsev, N.A., Adams, P.D., Jansen, L.E., et al. (2011). Dynamics of histone H3 deposition in vivo reveal a nucleosome gap-filling mechanism for H3.3 to maintain chromatin integrity. *Mol. Cell* 44, 928–941.
- Roberts, C., Sutherland, H.F., Farmer, H., Kimber, W., Halford, S., Carey, A., Brickman, J.M., Wynshaw-Boris, A., and Scambler, P.J. (2002). Targeted mutations in the Hira gene results in gastrulation defects and patterning abnormalities of mesoendodermal derivatives prior to early embryonic lethality. *Mol. Cell. Biol.* 22, 2318–2328.
- Roy, A.L. (2012). Biochemistry and biology of the inducible multifunctional transcription factor TFII-I: 10 years later. *Gene* 492, 32–41.
- Schwartzentruber, J., Korshunov, A., Liu, X.Y., Jones, D.T., Pfaff, E., Jacob, K., Sturm, D., Fontebasso, A.M., Quang, D.A., Tönjes, M., et al. (2012). Driver mutations in histone H3.3 and chromatin remodeling genes in paediatric glioblastoma. *Nature* 482, 226–231.
- Sherwood, P.W., Tsang, S.V., and Osley, M.A. (1993). Characterization of HIR1 and HIR2, two genes required for regulation of histone gene transcription in *Saccharomyces cerevisiae*. *Mol. Cell. Biol.* 13, 28–38.
- Szenker, E., Lacoste, N., and Almouzni, G. (2012). A developmental requirement for HIRA-dependent H3.3 deposition revealed at gastrulation in *Xenopus*. *Cell Rep.* 1, 730–740.
- Tagami, H., Ray-Gallet, D., Almouzni, G., and Nakatani, Y. (2004). Histone H3.1 and H3.3 complexes mediate nucleosome assembly pathways dependent or independent of DNA synthesis. *Cell* 116, 51–61.
- van der Heijden, G.W., Derijck, A.A., Pósfai, E., Giele, M., Pelczar, P., Ramos, L., Wansink, D.G., van der Vlag, J., Peters, A.H., and de Boer, P. (2007). Chromosome-wide nucleosome replacement and H3.3 incorporation during mammalian meiotic sex chromosome inactivation. *Nat. Genet.* 39, 251–258.
- Wu, G., Broniscer, A., McEachron, T.A., Lu, C., Paugh, B.S., Becksfors, J., Qu, C., Ding, L., Huether, R., Parker, M., et al.; St. Jude Children's Research Hospital-Washington University Pediatric Cancer Genome Project. (2012). Somatic histone H3 alterations in pediatric diffuse intrinsic pontine gliomas and non-brainstem glioblastomas. *Nat. Genet.* 44, 251–253.
- Yang, J.H., Song, Y., Seol, J.H., Park, J.Y., Yang, Y.J., Han, J.W., Youn, H.D., and Cho, E.J. (2011). Myogenic transcriptional activation of MyoD mediated by replication-independent histone deposition. *Proc. Natl. Acad. Sci. USA* 108, 85–90.